

# Chapter 6

## Group 13

### 6.1 The Group 13 Elements<sup>1</sup>

Table 6.1 lists the derivation of the names of the Group 13 (IIIA) elements.

Element	Symbol	Name
Boron	B	From the Arabic word <i>buraq</i> or the Persian word <i>burah</i> for the mineral <i>borax</i>
Aluminium (Aluminum)	Al	From <i>alum</i>
Gallium	Ga	From Named after the Latin word for France (Gaul) <i>Gallia</i>
Indium	In	Latin <i>rubidus</i> meaning <i>deepest red</i>
Thalium	Tl	From the Latin <i>thallus</i> meaning <i>sprouting green twig</i>

**Table 6.1:** Derivation of the names of each of the alkali metal elements.

NOTE: Aluminium is the international spelling standardized by the IUPAC, but in the United States it is more commonly spelled as aluminum.

#### 6.1.1 Discovery

##### 6.1.1.1 Boron

Borax (a mixture of  $\text{Na}_2\text{B}_4\text{O}_7 \cdot 4\text{H}_2\text{O}$  and  $\text{Na}_2\text{B}_4\text{O}_7 \cdot 10\text{H}_2\text{O}$ ) was known for thousands of years. In Tibet it was known by the Sanskrit name of *tinca*. Borax glazes were used in China in 300 AD, and the writings of the Arabic alchemist Geber (Figure 6.1) appear to mention it in 700 AD. However, it is known that Marco Polo brought some borax glazes back to Italy in the 13th century. In 1600 Agricola (Figure 6.2) in his treatise *De Re Metallica* reported the use of borax as a flux in metallurgy.

<sup>1</sup>This content is available online at <<http://cnx.org/content/m32149/1.3/>>.



**Figure 6.1:** A drawing of the *father of chemistry* Abu Musa Jābir ibn Hayyān al azdi known by Geber; the Latinized form of Jabir (721 - 815). Geber was a chemist and alchemist, astronomer and astrologer, engineer, geologist, philosopher, physicist, and pharmacist and physician.

---



**Figure 6.2:** A painting of German author Georg Bauer (1494 - 1555), whose pen-name was the Latinized Georgius Agricola, was most probably the first person to be environmentally conscious.

---

Boron was not recognized as an element until its isolation by Sir Humphry Davy (Figure 6.3), Joseph Louis Gay-Lussac (Figure 6.4) and Louis Jacques Thénard (Figure 6.5) in 1808 through the reaction of boric

acid and potassium. Davy called the element *boracium*. Jöns Jakob Berzelius (Figure 6.6) identified boron as an element in 1824.

---



**Figure 6.3:** British chemist and inventor Sir Humphry Davy FRS (1778 - 1829).

---



**Figure 6.4:** French chemist and physicist Joseph Louis Gay-Lussac (1778 -1850).

---



**Figure 6.5:** French chemist Louis Jacques Thénard (1777 - 1857).

---



**Figure 6.6:** Swedish chemist Friherre Jöns Jacob Berzelius (1779 - 1848).

---

### 6.1.1.2 Aluminum

Ancient Greeks and Romans used aluminum salts as dyeing mordants and as astringents for dressing wounds; alum ( $\text{KAl}(\text{SO}_4)_2 \cdot 12\text{H}_2\text{O}$ ) is still used as a styptic (an antihæmorrhagic agent). In 1808, Sir Humphry Davy (Figure 6.3) identified the existence of a metal base of alum, which he at first termed *alumium* and later aluminum.

The metal was first produced in 1825 (in an impure form) by Hans Christian Ørsted (Figure 6.7) by the reaction of anhydrous aluminum chloride with potassium amalgam. Friedrich Wöhler (Figure 6.8) repeated the experiments of Ørsted but suggested that Ørsted had only isolated potassium. By the use of potassium, (6.1), he is credited with isolating aluminum in 1827. While Wöhler is generally credited with isolating aluminum, Ørsted should also be given credit.



**Figure 6.7:** Danish physicist and chemist Hans Christian Ørsted (1777 - 1851).

---

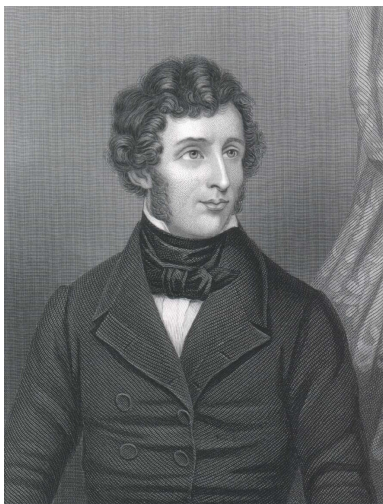


**Figure 6.8:** German chemist Friedrich Wöhler (1800 - 1882) also known for his synthesis of urea and, thus, the founding of the field of natural products synthesis.

---

In 1846 Henri Deville (Figure 6.9) improved Wöhler's method, and described his improvements in particular the use of sodium in place of the expensive potassium



**Figure 6.9:** French chemist Henri Etienne Saint-Claire Deville (1818 - 1881).

---

### 6.1.1.3 Gallium

The element gallium was predicted, as eka-aluminum, by Mendeleev (Figure 6.10) in 1870, and subsequently discovered by Lecoq de Boisbaudran (Figure 6.11) in 1875; in fact de Boisbaudran had been searching for the missing element for some years, based on his own independent theory. The first experimental indication of gallium came with the observation of two new violet lines in the spark spectrum of a sample deposited on zinc. Within a month of these initial results de Boisbaudran had isolated 1 g of the metal starting from several hundred kilograms of crude zinc blende ore. The new element was named in honor of France (Latin *Gallia*), and the striking similarity of its physical and chemical properties to those predicted by Mendeleev did much to establish the general acceptance of the periodic Law; indeed, when de Boisbaudran first stated that the density of Ga was  $4.7 \text{ g cm}^{-3}$  rather than the predicted  $5.9 \text{ g/cm}^3$ , Mendeleev wrote to him suggesting that he redetermine the value (the correct value is  $5.904 \text{ g/cm}^3$ ).

---

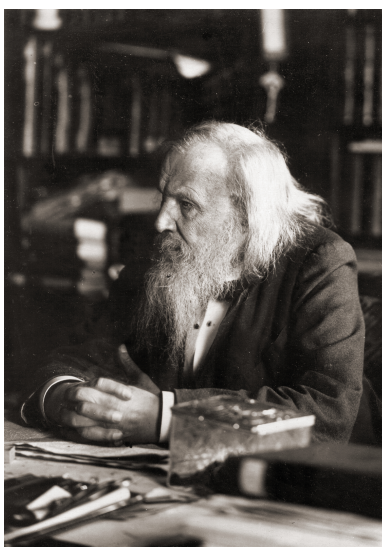


**Figure 6.10:** Russian chemist and inventor Dmitri Ivanovich Mendeleev (1834 – 1907).

---



**Figure 6.11:** French chemist Paul Émile (François) Lecoq de Boisbaudran (1838 – 1912).

---

#### 6.1.1.4 Indium

While testing ores from the mines around Freiberg, Saxony, Ferdinand Reich (Figure 6.12) and Hieronymus Theodor Richter (Figure 6.13) when they dissolved the minerals pyrite, arsenopyrite, galena and sphalerite in hydrochloric acid, and since it was known that ores from that region contained thallium they searched for the green emission lines by spectroscopy. Although the green lines were absent, a blue line was present in the spectrum. As no element was known with a bright blue emission they concluded that a new element was present in the minerals. They named the element with the blue spectral line indium. Richter went on to isolate the metal in 1864.



**Figure 6.12:** German chemist Ferdinand Reich (1799 - 1882).

---



**Figure 6.13:** German chemist Hieronymus Theodor Richter (1824 - 1898).

---

#### 6.1.1.5 Thallium

After the publication of their improved method of flame spectroscopy by Robert Bunsen (Figure 6.14) and Gustav Kirchhoff (Figure 6.15) this method became an accepted method to determine the composition of minerals and chemical products. Two chemists, William Crookes (Figure 6.16) and Claude-Auguste Lamy, both started to use the new method and independently employed it in their discovery of thallium.



**Figure 6.14:** German chemist Robert Wilhelm Eberhard Bunsen (1811 - 1899).

---

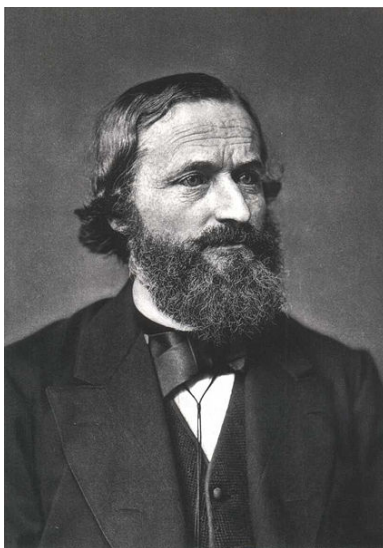


**Figure 6.15:** German physicist Gustav Robert Kirchhoff (1824 - 1887).

---

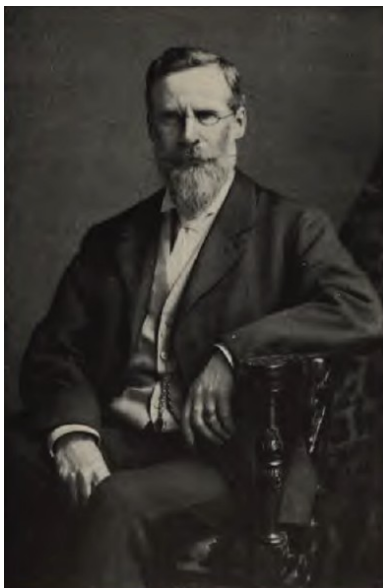


**Figure 6.16:** English chemist and physicist Sir William Crookes, FRS (1832 –1919) attended the Royal College of Chemistry (now Imperial College) in London.

---

Crookes was making spectroscopic determinations on selenium compounds deposited in the lead chamber of a sulfuric acid production plant near Tilkerode in the Harz mountains. Using a similar spectrometer to Crookes', Lamy was determining the composition of a selenium-containing substance that was deposited during the production of sulfuric acid from pyrite. Using spectroscopy both researchers both observed a new green line the atomic absorption spectrum and assigned it to a new element. Both set out to isolate the new element. Fortunately for Lamy, he had received his material in larger quantities and thus he was able to isolate sufficient quantities of thallium to determine the properties of several compounds and prepare a small ingot of metallic thallium. At the same time Crookes was able to isolate small quantities of elemental thallium and determine the properties of a few compounds. The claim by both scientists resulted in significant controversy during 1862 and 1863; interestingly this ended when Crookes was elected Fellow of the Royal Society in June 1863.

### 6.1.2 Abundance

The abundance of the Group 13 elements is given in Table 6.2. Aluminum is the most abundant metal in the Earth's crust and is found in a wide range of minerals. While boron is not as common it is also found in a range of borate minerals. In contrast, gallium, indium, and thallium are found as impurities in other minerals. In particular indium and thallium are found in sulfide or selenide mineral rather than oxides, while gallium is found in both sulfides ( $\text{ZnS}$ ) and oxides (bauxite). Although indium and thallium minerals are known, they are rare: indite ( $\text{FeIn}_2\text{S}_4$ ), lorandite ( $\text{TlAsS}_2$ ), crookesite ( $\text{Cu}_7\text{TlSe}_4$ ).

Element	Terrestrial abundance (ppm)
B	10 (Earth's crust), 20 (soil), 4 (sea water)
Al	82,000 (Earth's crust), 100,000 (soil), $5 \times 10^{-4}$ (sea water)
Ga	18 (Earth's crust), 28 (soil), $30 \times 10^{-6}$ (sea water)
In	0.1 (Earth's crust), 0.01 (soil), $0.1 \times 10^{-6}$ (sea water)
Tl	0.6 (Earth's crust), 0.2 (soil), $10 \times 10^{-6}$ (sea water)

**Table 6.2:** Abundance of Group 13 elements.

### 6.1.3 Isotopes

The naturally abundant isotopes of the Group 13 elements are listed in Table 6.3. Thallium has 25 isotopes that have atomic masses that range from 184 to 210. Thallium-204 is the most stable radioisotope, with a half-life of 3.78 years.

Isotope	Natural abundance (%)
Boron-10	19.9
Boron-11	80.1
Aluminum-27	100
Gallium-69	60.11
Gallium-71	39.89
Indium-113	4.3
Indium-115	95.7
Thallium-203	29.52
Thallium-205	70.48

**Table 6.3:** Abundance of the major isotopes of the Group 13 elements.

The Group 13 elements offer potential as NMR nuclei (Table 6.4). In particular  $^{11}\text{B}$  and  $^{27}\text{Al}$  show promise for characterization in both solution and solid state.

Isotope	Spin	Natural abundance (%)	Quadrupole moment ( $10^{-30} \text{ m}^2$ )	NMR frequency (MHz) at a field of 2.3488 T	Reference
<i>continued on next page</i>					

Boron-10	3	19.58	8.459	-10.746	BF <sub>3</sub> .Et <sub>2</sub> O
Boron-11	<sup>3</sup> / <sub>2</sub>	80.42	4.059	-32.084	BF <sub>3</sub> .Et <sub>2</sub> O
Aluminum-27	<sup>5</sup> / <sub>2</sub>	100	14.66	-26.057	Al(NO <sub>3</sub> ) <sub>3</sub>
Gallium-69	<sup>3</sup> / <sub>2</sub>	60.4	17.1	-24.003	Ga(NO <sub>3</sub> ) <sub>3</sub>
Gallium-71	<sup>3</sup> / <sub>2</sub>	39.6	10.7	-30.495	Ga(NO <sub>3</sub> ) <sub>3</sub>
Indium-113	<sup>9</sup> / <sub>2</sub>	4.28	79.9	-21.866	In(NO <sub>3</sub> ) <sub>3</sub>
Indium-115	<sup>9</sup> / <sub>2</sub>	95.72	81.0	-21.914	In(NO <sub>3</sub> ) <sub>3</sub>

**Table 6.4:** Isotopes of Group 13 elements for NMR spectroscopy.

### 6.1.4 Industrial production

Borax is mined as a mixture of Na<sub>2</sub>B<sub>4</sub>O<sub>7</sub>.4H<sub>2</sub>O and Na<sub>2</sub>B<sub>4</sub>O<sub>7</sub>.10H<sub>2</sub>O. Acidification gives boric acid, B(OH)<sub>3</sub>, which can be reduced with sodium amalgam (Na/Hg) to give amorphous boron. Pure boron can be prepared by reducing boron halides (e.g., BF<sub>3</sub> and BCl<sub>3</sub>) with hydrogen at high temperatures. Ultrapure boron, for the use in semiconductor industry, is produced by the decomposition of diborane (B<sub>2</sub>H<sub>6</sub>) and then further purified with the zone melting or Czochralski processes.

The only two economic sources for gallium are as byproduct of aluminum and zinc production. Extraction during the Bayer process followed by mercury cell electrolysis and hydrolysis of the amalgam with sodium hydroxide leads to sodium gallate. Electrolysis then gives gallium metal.

The lack of indium mineral deposits and the fact that indium is enriched in sulfides of lead, tin, copper, iron and zinc, makes the zinc production the main source for indium. The indium is leached from slag and dust of zinc production. Up until 1924, there was only about a gram of isolated indium on the planet, however, today worldwide production is currently greater 476 tons per year from mining and a 650 tons per year from recycling. This massive increase in demand is due to applications in LCD displays and solar cell applications.

#### 6.1.4.1 Aluminum

Due to aluminum's position as the most abundant metallic element in the Earth's crust (7.5 - 8.1%) and its enormous industrial importance warrants detailed discussion of its industrial production. Aluminum only appears in its elemental form in nature in oxygen-deficient environments such as volcanic mud. Ordinarily, it is found in a variety of oxide minerals.

In comparison to other metals aluminum is difficult to extract from its ores. Unlike iron, aluminum oxides cannot be reduced by carbon, and so purification is only possible on an economic scale using electrolysis. Prior to electrolysis purified aluminum oxide is obtained by refining bauxite in the process of developed by Karl Bayer (Figure 6.17).

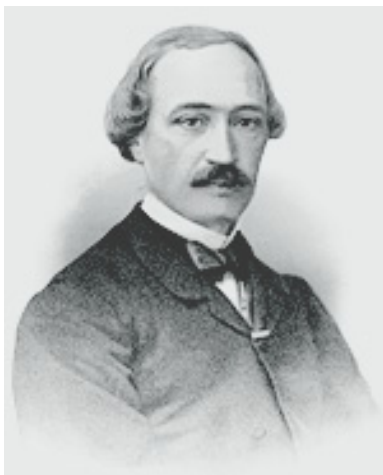


**Figure 6.17:** Austrian chemist Karl Josef Bayer (1847 –1904) whose father, Friedrich, founded the Bayer chemical and pharmaceutical company.

---

Bauxite, the most important ore of aluminum, contains only 30-50% alumina,  $\text{Al}_2\text{O}_3$ , the rest being a mixture of silica, iron oxide, and titanium dioxide. Thus, the alumina must be purified before it can be used as the oxide or refined into aluminum metal. In the Bayer process, bauxite is digested in hot (175 °C) sodium hydroxide (NaOH) solution (Figure 6.18). This converts the alumina to aluminum hydroxide,  $\text{Al}(\text{OH})_3$ , which dissolves in the hydroxide solution.



The other components do not dissolve and are filtered off (Figure 6.18). The hydroxide solution is cooled, and the dissolved aluminum hydroxide precipitates, which when heated to 1050 °C is calcined into alumina.



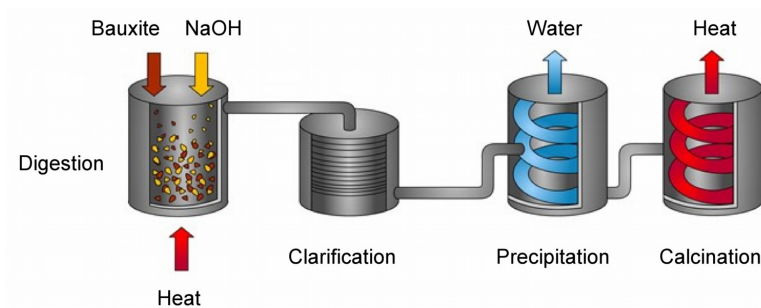


**Figure 6.18:** Schematic representation of the Bayer process. Copyright: Andrew Perchard, Alcan Aluminium UK and courtesy of Glasgow University Archives (2007).

---

Once a pure alumina is formed, it is dissolved in molten cryolite ( $\text{Na}_3\text{AlF}_6$ ) and reduced to the pure metal at elevated temperatures (950 - 980 °C) using the Hall-Hérout process, developed independently Charles Hall (Figure 6.19) and Paul Hérout (Figure 6.20).

---



**Figure 6.19:** American inventor and engineer Charles Martin Hall (1863 – 1914).

---



**Figure 6.20:** French scientist Paul (Louis-Toussaint) Héroult (1863 – 1914).

Both of the electrodes used in the electrolysis of aluminum oxide are carbon (Figure 6.21). The reaction at the cathode involves the reduction of the  $\text{Al}^{3+}$ , (6.5). The aluminum metal then sinks to the bottom and is tapped off, where it is usually cast into large blocks called aluminum billets.

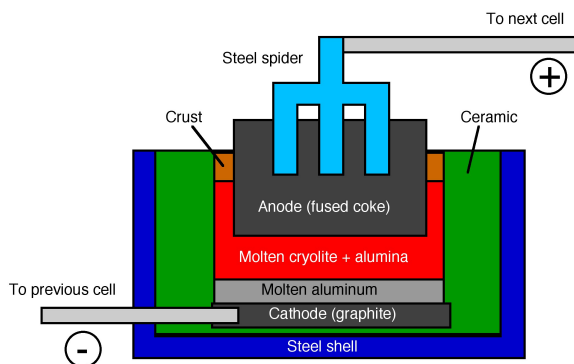


**Figure 6.21:** Schematic of the Hall-Héroult cell.

At the anode oxygen is formed, (6.6), where it reacts with the carbon anode is then oxidized to carbon

dioxide, (6.7). The anodes must be replaced regularly, since they are consumed. While the cathodes are not oxidized they do erode due to electrochemical processes and metal movement.



Although the Hall-Héroult process consumes a lot of energy, alternative processes have always found to be less economically and ecologically viable.

### 6.1.5 Physical properties

Table 6.5 summarizes the physical properties of the Group 13 elements. While, aluminum, indium, and thallium have typical metal properties, gallium has the largest liquid range of any element. Boron exists as a molecular compound in the solid state, hence its high melting point.

Element	Mp (°C)	Bp (°C)	Density (g/cm <sup>3</sup> )
B	2300	3658	2.3
Al	661	2467	2.7
Ga	30	2403	5.9 (solid), 6.1 (liquid)
In	156	2080	7.3
Tl	304	1457	11.9

**Table 6.5:** Selected physical properties of the Group 13 elements.

### 6.1.6 Bibliography

- C. M. Hall. *Process of reducing aluminum from its fluoride salts by electrolysis*. US Patent 400,664 (1886).
- L. B. Alemany, S. Steuernagel, J.-P. Amoureux, R. L. Callender, and A. R. Barron. *Solid State Nuclear Magnetic Resonance*, 1999, **14**, 1.
- L. B. Alemany, R. L. Callender, A. R. Barron, S. Steuernagel, D. Iuga, and A. P. M. Kentgens, *J. Phys. Chem., B.*, 2000, **104**, 11612.
- M. Bishop, N. Shahid, J. Yang, and A. R. Barron, *Dalton Trans.*, 2004, 2621.

## 6.2 Trends for the Group 13 Compounds<sup>2</sup>

Boron is a non-metal with metalloidal tenancies. The higher ionization energies for boron than for its other Group homologs are far more than would be compensated by lattice energies, and thus, the B<sup>3+</sup> ion plays no part in the chemistry of boron, and its chemistry is dominated by the formation of covalent compounds. In contrast, the elements aluminum through thallium each has a low electronegativity and the chemistry of their compounds reflects this characteristic. Each of the Group 13 metals forms both covalent compounds and ionic coordination complexes.

All of the Group 13 (IIIA) elements have a valence shell electron configuration of  $ns^2np^1$ . As a consequence all of the Group 13 elements for compounds in which they adopt a +3 oxidation state. While the lighter

<sup>2</sup>This content is available online at <<http://cnx.org/content/m32522/1.2/>>.

elements do form compounds with lower oxidation state, they are not the norm; however, the +1 oxidation state is more prevalent for the heavier elements in particular thallium. The rationale for this is described as the *inert pair effect*. The inert pair effect is usually explained by the energy of the  $ns$  orbital is lower making it harder to ionize and stabilizing a  $ns^2np^0$  valence shell. However, as may be seen from Table 6.6 the sum of the second and third ionization enthalpies is lower for indium (4501 kJ/mol), than for gallium (4916 kJ/mol), but with thallium intermediate (4820 kJ/mol). The true source of the inert pair effect is that the lower bond strengths observed for the heavier elements (due to more diffuse orbitals and therefore less efficient overlap) cannot compensate for the energy needed to promote the  $ns^2$  electrons. For example, the bond energies for gallium, indium, and thallium in  $MCl_3$  are 242, 206, and 153 kJ/mol, respectively. It has also been suggested that relativistic effects make a contribution to the inert pair effect.

Ionization enthalpy (kJ/mol)	Al	Ga	In	Tl
1	576.4	578.3	558.1	589.0
2	1814.1	1969.3	1811.2	1958.7
3	2741.4	2950.0	2689.3	2868.8

**Table 6.6:** Summary of first three ionization enthalpies for the Group 13 metals.

In summary, it may be stated that while the chemistry of gallium, indium and thallium is very similar, that of aluminum is slightly different, while boron's chemistry is very different from the rest of the Group.

A second effect is noticed in the transition from aluminum, to gallium, to indium. Based upon their position in the Group it would be expected that the ionic radius and associated lattice parameters should follow the trend:

$$Al < Ga < In < Tl \quad (6.8)$$

However, as may be seen from Table 6.7 the values for gallium are either the same as, or smaller, than that of aluminum. In a similar manner, the covalent radius and covalent bond lengths as determined by X-ray crystallography for a range of compounds (Table 6.8).

Element	Phosphide lattice parameter (Å)	Arsenide lattice parameter (Å)
Al	5.4635	5.6600
Ga	5.4505	5.6532
In	5.8687	6.0583

**Table 6.7:** Table. Lattice parameter ( $a$ ) for zinc blende forms of the Group 13 phosphides and arsenides. Data from *Semiconductors: Group IV Elements and III-V Compounds*, Ed. O. Madelung, Springer-Verlag, Berlin (1991).

Element	M-C (Å)	M-N (Å)	M-O (Å)	M-Cl (Å)
Al	1.96 – 2.02	2.03 – 2.19	1.74 – 1.93	2.09 – 2.11
Ga	1.97 – 2.01	1.95 – 2.12	1.89 – 1.94	2.12 – 2.23
In	2.14 – 2.17	2.23 – 2.31	2.19 – 2.20	2.39 – 2.47

**Table 6.8:** Comparative crystallographically determined bond lengths.

Gallium is significantly smaller than expected from its position within the Group 13 elements (Table 6.9). The rationale for this may be attributed to an analogous effect as seen in the *lanthanide contraction* observed for the lanthanides and the 3<sup>rd</sup> row of transition elements. In multi-electron atoms, the decrease in radius brought about by an increase in nuclear charge is partially offset by increasing electrostatic repulsion among electrons. In particular, a “shielding effect” results when electrons are added in outer shells, electrons already present shield the outer electrons from nuclear charge, making them experience a lower effective charge on the nucleus. The shielding effect exerted by the inner electrons decreases in the order  $s > p > d > f$ . As a sub-shell is filled in a period the atomic radius decreases. This effect is particularly pronounced in the case of lanthanides, as the  $4f$  sub-shell is not very effective at shielding the outer shell ( $n = 5$  and  $n = 6$ ) electrons. However, a similar, but smaller effect should be observed with the post-transition metal elements, i.e., gallium. This is indeed observed (Table 6.9).

Element	Covalent radius (Å)	Ionic radius (Å)
Aluminum	1.21	0.53
Gallium	1.22	0.62
Indium	1.42	0.80
Iron (low spin)	1.32	0.55
Iron (high spin)	1.52	0.64

**Table 6.9:** Comparison of the covalent and ionic radii of Group 13 elements.

The anomalous size of gallium has two positive effects.

1. The similarity in size of aluminum and gallium means that their Group 15 derivatives have near identical lattice parameters (Table 6.7). This allows for both epitaxial growth of one material on the other, and also the formation of ternary mixtures (i.e.,  $\text{Al}_x\text{Ga}_{1-x}\text{As}$ ) with matched lattice parameters. The ability to grow heterojunction structures of Group 13-15 compounds (III-V) is the basis for the fabrication of a wide range of important optoelectronic devices, including: LEDs and laser diodes.
2. The similarity in size of gallium(III) to iron(III) (Table 6.9) means that gallium can substitute iron in a range of coordination compounds without alteration of the structure. Because of a similar size and charge as  $\text{Fe}^{3+}$ ,  $\text{Ga}^{3+}$  is widely used as a non-redox-active  $\text{Fe}^{3+}$  substitute for studying metal complexation in proteins and bacterial populations.

### 6.2.1 Bibliography

- K. S. Pitzer, *Acc. Chem. Res.*, 1979, **12**, 271.
- K. D. Weaver, J. J. Heymann, A. Mehta, P. L. Roulhac, D. S. Anderson, A. J. Nowalk, P. Adhikari, T. A. Mietzner, M. C. Fitzgerald, and A. L. Crumbliss, *J. Biol. Inorg. Chem.*, 2008, **13**, 887.
- *Semiconductors: Group IV Elements and III-V Compounds*, Ed. O. Madelung, Springer-Verlag, Berlin (1991).

## 6.3 Borides<sup>3</sup>

The non-metallic nature of boron means that it makes a number of binary compounds with elements more electropositive than itself (i.e., metals). These compounds are called, *borides*, and some are also formed

<sup>3</sup>This content is available online at <<http://cnx.org/content/m32447/1.2/>>.

with metalloids as well (e.g., arsenic). In this regard, borides may be considered similar to carbides, silicides, and some phosphides.

Borides are prepared in a number of ways, however, direct combination of the elements, (6.9), is the simplest. Other routes include, electrolysis of the fused salts, and the reduction of the metal oxide with a mixture of carbon and boron carbide.



Metal borides are generally refractory in character and chemically inert, while they often have properties better than that of the constituent elements. For example, the thermal conductivity of  $TiB_2$  is about ten times greater than that of titanium, and the melting point is significantly higher (Table 6.10).

Element	Melting point ( $^{\circ}C$ )	Boride	Melting point ( $^{\circ}C$ )
Ti	1725	$TiB_2$	3225
Zr	1855	$ZrB_2$	2990
Hf	2233	$HfB_2$	3100

**Table 6.10:** The melting points of Group 4 metals and their borides.

The structures of metal borides depends on the M:B ratio. Borides with an isolated boron atom have a low B:M ratio:  $M_4B$ ,  $M_3B$ ,  $M_2B$ ,  $M_5B_2$ , and  $M_7B_3$ . In such compounds the boron atom is normally in a triangular-prismatic or square-antiprismatic hole in a metal lattice. Borides with equal or near equal metal and boron ratio have structures with either pairs of boron atoms (as in  $V_3B_2$ ), single boron chains (seen in all MB compounds), or double boron chains (observed for many  $M_3B_4$  compounds). Increasing the boron content results in two-dimensional structures. For example,  $MB_2$  usually consists of alternate hexagonal layers of metal and boron (Figure 6.22). Finally, boron rich borides (e.g.,  $MB_4$ ,  $MB_6$ , and  $MB_{12}$ ) all have three-dimensional structures.

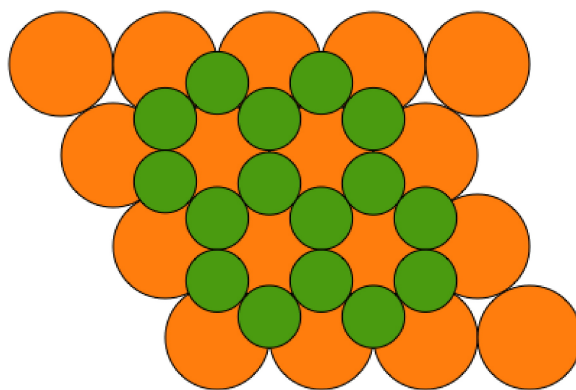


**Figure 6.22:** Alternate layers of metal atoms (large circles) and boron (small circles) in  $MB_2$ .

## 6.4 Hydrides

### 6.4.1 Boron Hydrides<sup>4</sup>

#### 6.4.1.1 Borane and diborane

Borane ( $\text{BH}_3$ ) formed in the gaseous state from decomposition of other compounds, (6.11), but cannot be isolated except as a Lewis acid-base complex, (6.10). As such many borane adducts are known.



In the absence of a Lewis base the dimeric diborane ( $\text{B}_2\text{H}_6$ ) is formed. Diborane is generally synthesized by the reaction of  $\text{BF}_3$  with a hydride source, such as  $\text{NaBH}_4$ , (6.13), or  $\text{LiAlH}_4$ , (6.12).



The structure of diborane (Figure 6.23a) is considered to be electron deficient, and has been confirmed by IR spectroscopy and electron diffraction. The four terminal B-H bonds are normal covalent bonds, however, the bridging B-H-B unit consists of two three-centered two-electron bonds, each ordinarily considered to be formed by the combination of two boron  $sp^3$  orbitals and one hydrogen  $s$  orbital (Figure 6.23b). However, a consideration of the H-B-H bond angle associated with the terminal hydrides ( $120^\circ$ ) it is perhaps better to consider the  $\text{BH}_2$  fragment to be  $sp^2$  hybridized, and the B-H-B bridging unit to be a linear combination of one  $sp^2$  orbital and one  $p$  orbital from each boron atom with the two hydrogen  $s$  orbitals. Diborane represents the archetypal electron deficient dimeric compound, of which  $\text{Al}_2\text{Me}_3$  is also a member of this class of electron deficient molecules.

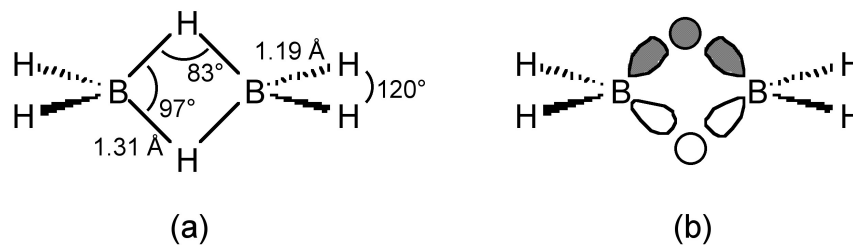


**Figure 6.23:** The structure (a) and the typical view of the three-centered two-electron bonds (b) in diborane,  $\text{B}_2\text{H}_6$ .

$\text{B}_2\text{H}_6$  is spontaneously and highly exothermically inflammable above  $25^\circ\text{C}$  ( $\Delta H = -2137.7 \text{ kJ/mol}$ ), (6.14). It is often used as one of a range of solvate forms for safety for both its flammability and toxicity.



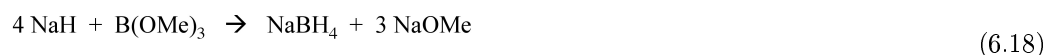
<sup>4</sup>This content is available online at <<http://cnx.org/content/m35228/1.1/>>.

Most reactions of diborane involve the cleavage of the dimeric structure. Hydrolysis of diborane yields boric acid, (6.15), while alcoholysis yields the appropriate borate ester, (6.16). Diborane reacts with Lewis bases to form the appropriate Lewis acid-base complex, (6.17).



#### 6.4.1.1.1 Borohydride

The borohydride anion (or more properly the tetrahydridoborate anion),  $\text{BH}_4^-$ , can be considered as the Lewis acid-base complex between borane and  $\text{H}^-$ . A typical synthesis involves the reaction of a borate ester with a hydride source, (6.18).



Sodium borohydride is a stable white crystalline solid that is stable in dry air and is non-volatile. The boron in borohydride ( $\text{BH}_4^-$ ) is tetrahedral. Although it is insoluble in  $\text{Et}_2\text{O}$ , it is soluble in water (in which it reacts slowly), THF, ethylene glycol, and pyridine. Interestingly,  $\text{NaBH}_4$  reacts rapidly with MeOH, but dissolves in EtOH. Sodium borohydride has extensive uses in organic chemistry as a useful reducing agent in which it donates a hydride ( $\text{H}^-$ ).

#### 6.4.1.2 Higher boranes

Higher boron hydrides contain, in addition to the bridging B-H-B unit, one or more B-B bonds. The higher boranes are usually formed by the thermal decomposition of diborane, (6.19) and (6.20).



These higher boranes have 'open' cluster structures, e.g., Figure 6.24 - Figure 6.26. Tetraborane, or to be more precise tetraborane(10) or *arachno*- $\text{B}_4\text{H}_{10}$ , is a foul-smelling toxic gas. Pentaborane (9) is a toxic liquid (with a distinctive garlic odor) that can detonate in air, and like decaborane(14) was at one time considered as a potential rocket fuel. Because simple boron compounds burn with a characteristic green flame, the nickname for these fuels in the US military was *Green Dragon*. Problems with using boranes as a fuel included their toxicity and the characteristic of bursting into flame on contact with the air; furthermore, the exhaust would also be toxic. The US program resulted in a stockpile of borane fuels, in particular pentaborane(9), which was not destroyed until 2000. The system for the destroying the boranes was appropriately known as *Dragon Slayer*.

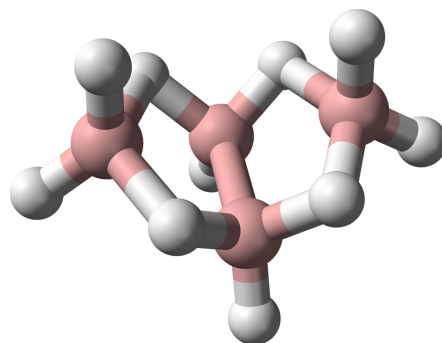


**Figure 6.24:** The molecular structure of tetraborane(10),  $B_4H_{10}$ . Boron atoms are represented by pink spheres, and hydrogen by white spheres.

---

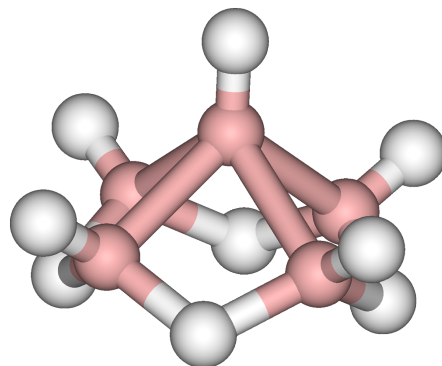


**Figure 6.25:** The molecular structure of pentaborane(9),  $B_5H_9$ . Boron atoms are represented by pink spheres, and hydrogen by white spheres.

---

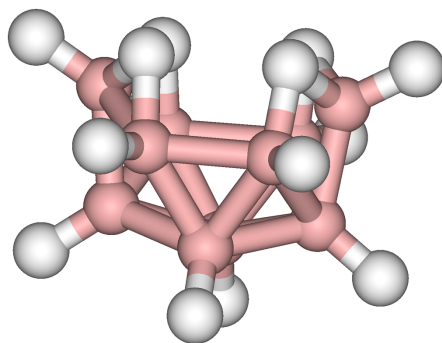


**Figure 6.26:** The molecular structure of decaborane(14),  $B_{10}H_{14}$ . Boron atoms are represented by pink spheres, and hydrogen by white spheres.

---

#### 6.4.1.3 Bibliography

- D. F. Gaines, *Acc. Chem. Res.*, 1973, **6**, 416.
- C. E. Housecroft, *Boranes and metalboranes: structure, bonding and reactivity*, Ellis Horwood, Chichester (1990).
- C. F. Lane, *Chem. Rev.*, 1976, **76**, 773.

#### 6.4.2 Wade's Rules<sup>5</sup>

Ken Wade (Figure 6.27) developed a method for the prediction of shapes of borane clusters; however, it may be used for a wide range of substituted boranes (such as carboranes) as well as other classes of cluster compounds.

---

<sup>5</sup>This content is available online at <<http://cnx.org/content/m32846/1.2/>>.

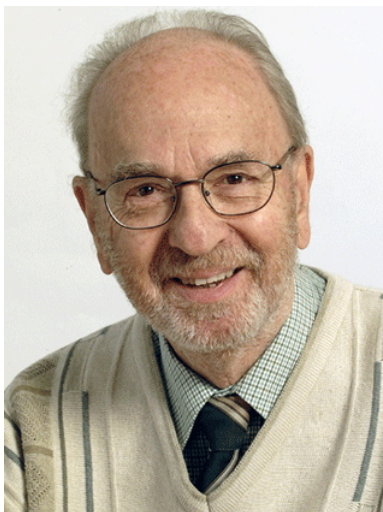


**Figure 6.27:** Chemist Ken Wade FRS.

---

Wade's rules are used to rationalize the shape of borane clusters by calculating the total number of skeletal electron pairs (SEP) available for cluster bonding. In using Wade's rules it is key to understand structural relationship of various boranes (Figure 6.28).

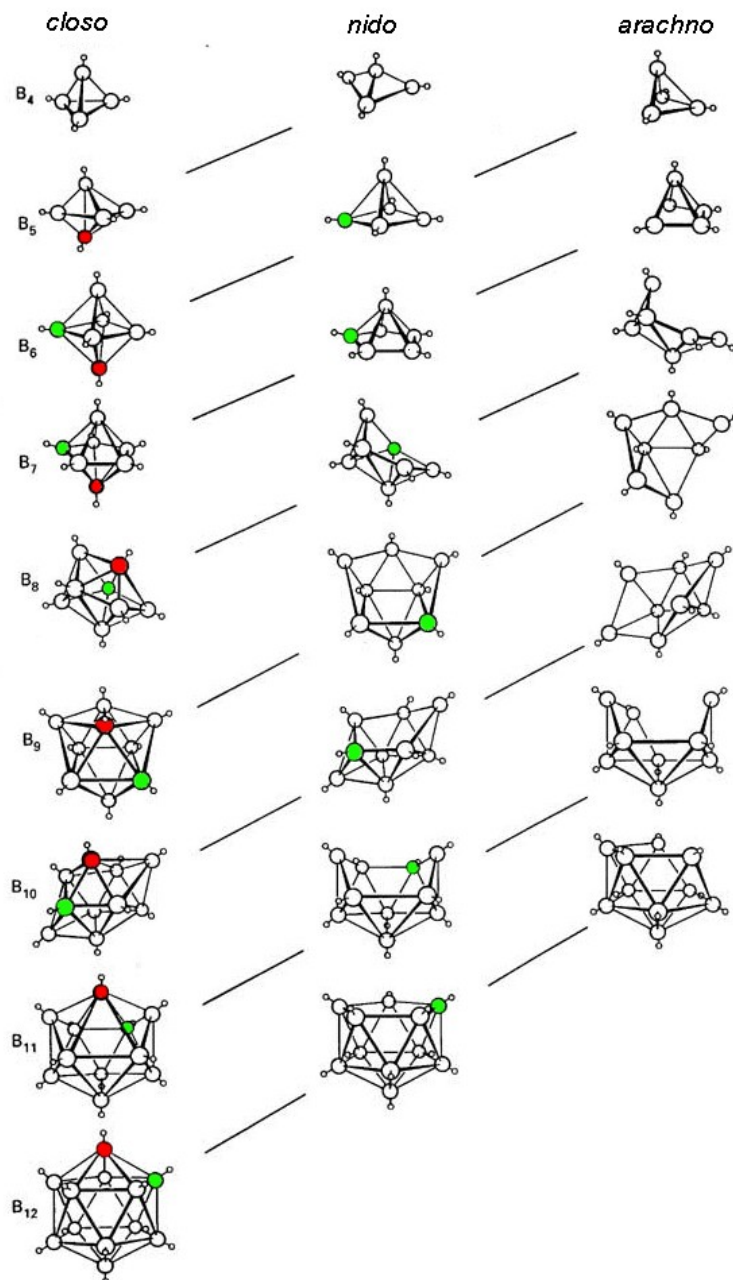


**Figure 6.28:** Structural relationship between *closo*, *nido*, and *arachno* boranes (and hetero-substituted boranes). The diagonal lines connect species that have the same number of skeletal electron pairs (SEP). Hydrogen atoms except those of the B-H framework are omitted. The red atom is omitted first, the green atom removed second. Adapted from R. W. Rudolph, *Acc. Chem. Res.*, 1976, **9**, 446.

The general methodology to be followed when applying Wade's rules is as follows:

1. Determine the total number of valence electrons from the chemical formula, i.e., 3 electrons per B, and 1 electron per H.
2. Subtract 2 electrons for each B-H unit (or C-H in a carborane).
3. Divide the number of remaining electrons by 2 to get the number of skeletal electron pairs (SEP).
4. A cluster with  $n$  vertices (i.e.,  $n$  boron atoms) and  $n+1$  SEP for bonding has a *closo* structure.
5. A cluster with  $n-1$  vertices (i.e.,  $n-1$  boron atoms) and  $n+1$  SEP for bonding has a *nido* structure.
6. A cluster with  $n-2$  vertices (i.e.,  $n-2$  boron atoms) and  $n+1$  SEP for bonding has an *arachno* structure.
7. A cluster with  $n-3$  vertices (i.e.,  $n-3$  boron atoms) and  $n+1$  SEP for bonding has an *hypho* structure.
8. If the number of boron atoms (i.e.,  $n$ ) is larger than  $n+1$  SEP then the extra boron occupies a capping position on a triangular phase.

### Example 6.1

What is the structure of  $B_5H_{11}$ ?

1. Total number of valence electrons =  $(5 \times B) + (11 \times H) = (5 \times 3) + (11 \times 1) = 26$
2. Number of electrons for each B-H unit =  $(5 \times 2) = 10$
3. Number of skeletal electrons =  $26 - 10 = 16$
4. Number SEP =  $16/2 = 8$
5. If  $n+1 = 8$  and  $n-2 = 5$  boron atoms, then  $n = 7$
6. Structure of  $n = 7$  is pentagonal bipyramid (Figure 6.28), therefore  $B_5H_{11}$  is an *arachno* based upon a pentagonal bipyramid with two apexes missing (Figure 6.29).

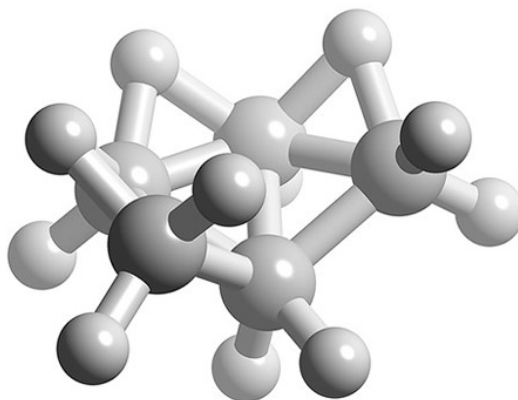


**Figure 6.29:** Ball and stick representation of the structure of  $B_5H_{11}$ .

### Example 6.2

What is the structure of  $B_5H_9$ ?

1. Total number of valence electrons =  $(5 \times B) + (9 \times H) = (5 \times 3) + (9 \times 1) = 24$
2. Number of electrons for each B-H unit =  $(5 \times 2) = 10$
3. Number of skeletal electrons =  $24 - 10 = 14$
4. Number SEP =  $14/2 = 7$
5. If  $n+1 = 7$  and  $n-1 = 5$  boron atoms, then  $n = 6$

6. Structure of  $n = 6$  is octahedral (Figure 6.28), therefore  $B_5H_9$  is a *nido* structure based upon an octahedral structure with one apex missing (Figure 6.30).

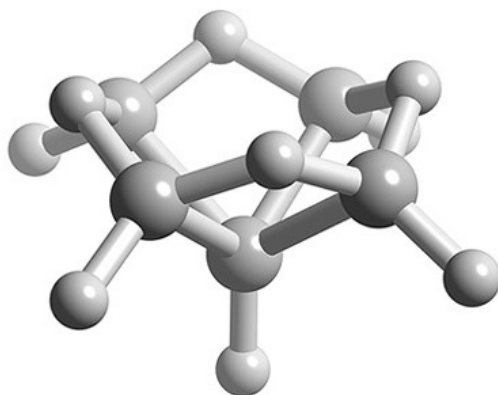


**Figure 6.30:** Ball and stick representation of the structure of  $B_5H_9$ .

#### Exercise 6.4.2.1

(Solution on p. 276.)

What is the structure of  $B_6H_6^{2-}$ ?

Table 6.11 provides a summary of borane cluster with the general formula  $B_nH_n^{x-}$  and their structures as defined by Wade's rules.

Type	Basic formula	Example	# of vertices	# of vacancies	# of e- in B + charge	# of bonding MOs
<i>Closo</i>	$B_nH_n^{2-}$	$B_6H_6^{2-}$	$n$	0	$3n + 2$	$n + 1$
<i>Nido</i>	$B_nH_n^{4-}$	$B_5H_9$	$n + 1$	1	$3n + 4$	$n + 2$
<i>Arachno</i>	$B_nH_n^{6-}$	$B_4H_{10}$	$n + 2$	2	$3n + 6$	$n + 3$
<i>Hypho</i>	$B_nH_n^{8-}$	$B_5H_{11}^{2-}$	$n + 3$	3	$3n + 8$	$n + 4$

**Table 6.11:** Wade's rules for boranes.

#### 6.4.2.1 Bibliography

- R. W. Rudolph, *Acc. Chem. Res.*, 1976, **9**, 446.
- K. Wade, *Adv. Inorg. Chem. Radiochem.*, 1976, **18**, 1.

## 6.5 Oxides, Hydroxides, and Oxygen Donor Ligands

### 6.5.1 Trends for the Oxides of the Group 13 Elements<sup>6</sup>

All of the Group 13 elements form a trivalent oxide ( $M_2O_3$ ). The chemical properties of the oxides follow the trend acidic to basic going down the Group (Table 6.12). The physical properties are consistent with the electronegativities and covalent character in the M-O bonds. Thallium oxide is unique in that it decomposes above 100 °C to yield the thallium(I) oxide,  $Tl_2O$ . The other oxides are all stable to high temperatures.

Oxide	Color	Chemical property	Melting point (°C)
$B_2O_3$	White/colorless	Weak acid	450 (trigonal), 510 (tetrahedral)
$Al_2O_3$	White/colorless	Amphoteric	2072 ( $\alpha$ )
$Ga_2O_3$	White/colorless	Amphoteric	1900 ( $\alpha$ ), 1725 ( $\beta$ )
$In_2O_3$	Yellow	Weakly basic	1910
$Tl_2O_3$	Brown-black	Basic, oxidizing	100 (decomposes)

Table 6.12: Properties of the Group 13 oxides.

#### 6.5.1.1 Bibliography

- G. E. Jellison, Jr., L. W. Panek, P. J. Bray, and G. B. Rouse, Jr., *J. Chem. Phys.*, 1977, **66**, 802.

### 6.5.2 Boron Oxides, Hydroxides, and Oxyanions<sup>7</sup>

#### 6.5.2.1 Oxides

Boron oxide,  $B_2O_3$ , is made by the dehydration of boric acid, (6.21). It is a glassy solid with no regular structure, but can be crystallized with extreme difficulty. The structure consists of infinite chains of triangular  $BO_3$  unit (Figure 6.31). Boron oxide is acidic and reacts with water to reform boric acid, (6.21).



<sup>6</sup>This content is available online at <<http://cnx.org/content/m32460/1.1/>>.

<sup>7</sup>This content is available online at <<http://cnx.org/content/m32461/1.3/>>.

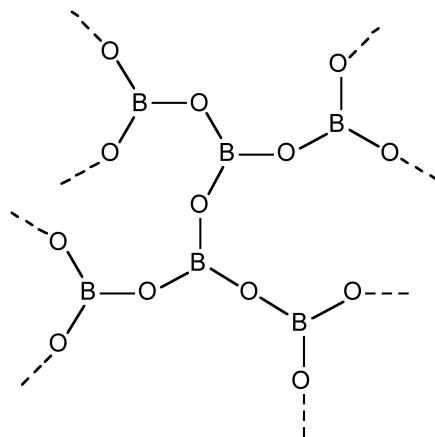


**Figure 6.31:** Glassy structure of  $B_2O_3$ .

The reaction of  $B_2O_3$  with hydroxide yields the metaborate ion, (6.22), whose planar structure (Figure 6.32) is related to metaboric acid. Boron oxide fuses with a wide range of metal and non-metal oxides to give borate glasses.

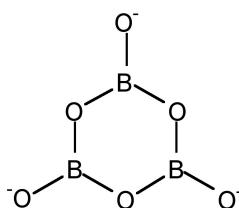


**Figure 6.32:** Structure of the metaborate anion,  $[B_3O_6]^{3-}$ .

### 6.5.2.2 Boric acid

Boric acid,  $B(OH)_3$ , usually obtained from the dissolution of borax,  $Na_2[B_4O_5(OH)_4]$ , is a planar solid with intermolecular hydrogen bonding forming a near hexagonal layered structure, broadly similar to graphite (Figure 6.33). The inter layer distance is 3.18 Å.

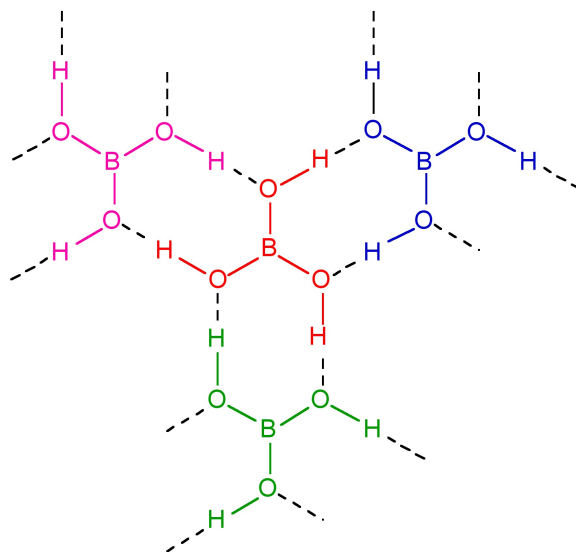


**Figure 6.33:** The hydrogen bonded structure of boric acid.

A summary of reactions of the reactivity of boric acid is shown in Figure 6.34.

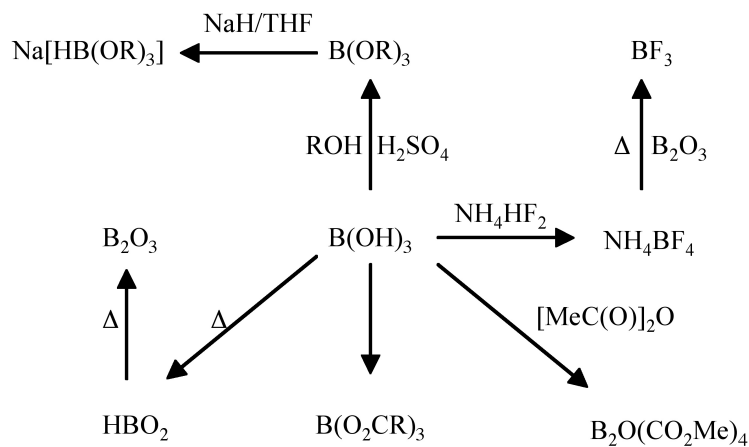


**Figure 6.34:** Selected reactions of boric acid. Adapted from F. A. Cotton and G. Wilkinson, *Advanced Inorganic Chemistry*, 4<sup>th</sup> Ed. Wiley Interscience (1980).

Upon dissolution of boric acid in water, boric acid does not act as a proton acid, but instead reacts as a

Lewis acid, (6.23).



The reaction may be followed by  $^{11}\text{B}$  NMR spectroscopy from the change in the chemical shift (Figure 6.35).

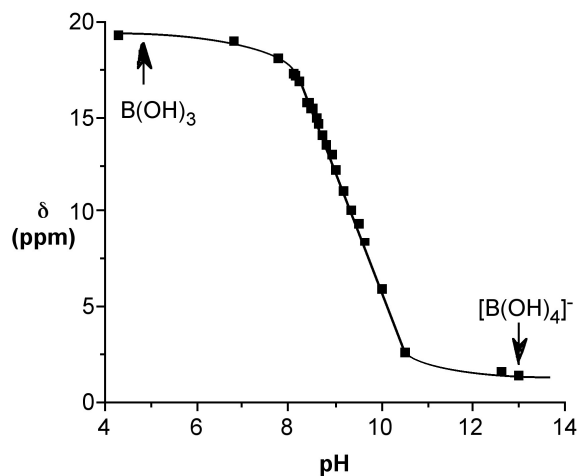
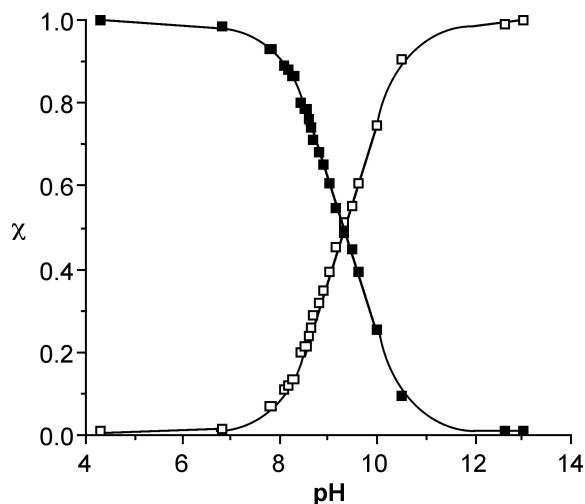


**Figure 6.35:** The  $^{11}\text{B}$  NMR chemical shift (ppm) of boric acid as a function of pH. Adapted from M. Bishop, N. Shahid, J. Yang, and A. R. Barron, *Dalton Trans.*, 2004, 2621.

Since the  $^{11}\text{B}$  NMR shift is directly proportional to the mole fraction of the total species present as the borate anion (e.g.,  $[\text{B(OH)}_4]^-$ ) the  $^{11}\text{B}$  NMR chemical shift at a given temperature,  $\delta_{(\text{obs})}$ , may be used to calculate both the mole fraction of boric acid and the borate anion, i.e., (6.24) and (6.25), respectively. Using these equations the relative speciation as a function of pH may be calculated for both boric acid (Figure 6.36). The pH at which a 50:50 mixture of acid and anion for boric acid is ca. 9.4.

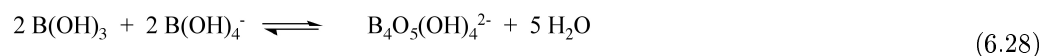
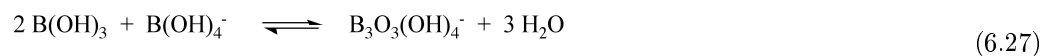
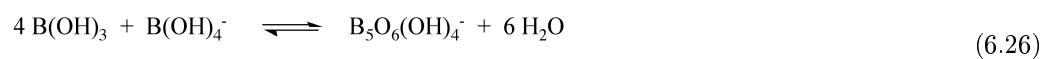
$$\chi_{(\text{acid})} = \frac{\delta_{(\text{obs})} - \delta_{(\text{anion})}}{\delta_{(\text{acid})} - \delta_{(\text{anion})}} \quad (6.24)$$

$$\chi_{(\text{anion})} = \frac{\delta_{(\text{acid})} - \delta_{(\text{obs})}}{\delta_{(\text{acid})} - \delta_{(\text{anion})}} \quad (6.25)$$



**Figure 6.36:** The mole fraction of acid (black squares) and anion (white squares) forms of boric acid as a function of pH. Adapted from M. Bishop, N. Shahid, J. Yang, and A. R. Barron, *Dalton Trans.*, 2004, 2621.

In concentrated solutions, the borate ion reacts further to form polyborate ions. The identity of the polyborate is dependent on the pH. With increasing pH,  $B_5O_6(OH)_4^-$ , (6.26),  $B_3O_3(OH)_4^-$ , (6.27), and  $B_4O_5(OH)_4^{2-}$ , (6.28), are formed. The structure of each borate is shown in Figure 6.37. Once the ratio of  $B(OH)_3$  to  $B(OH)_4^-$  is greater than 50%, only the mono-borate is observed.



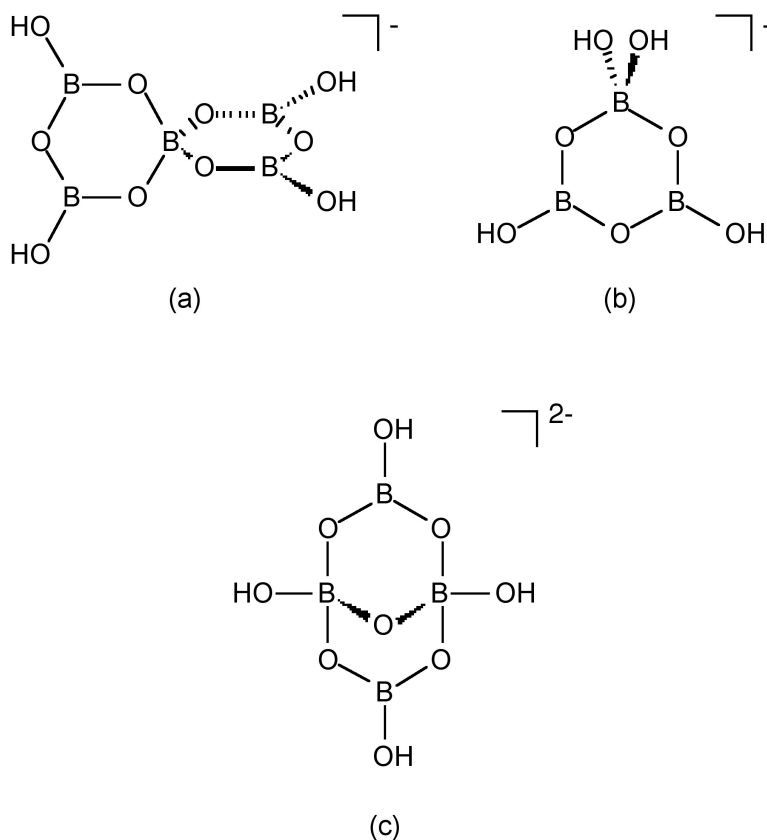


**Figure 6.37:** The structures of the borate anions (a)  $B_5O_6(OH)_4^-$ , (b)  $B_3O_3(OH)_4^-$ , and (c)  $B_4O_5(OH)_4^{2-}$ .

Borax, the usual mineral form of boric acid, is the sodium salt,  $Na_2[B_4O_5(OH)_4]$ , which upon dissolution in water re-equilibrates to  $B(OH)_3$ .

#### 6.5.2.2.1 Enough to make your hair curl

In 1906, a German hairdresser, Charles Nessler who was living in London, decided to help his sister who was fed-up with having to put her straight hair in curlers. While looking for a solution, Nessler noticed that a clothesline contracted in a wavy shape when it was wet. Nessler wound his sister's hair on cardboard tubes; then he covered the hair with borax paste. After wrapping the tubes with paper (to exclude air) he heated the entire mass for several hours. Removing the paper and tubes resulted in curly hair. After much trial and error (presumably at his sister's discomfort) Nessler perfected the method by 1911, and called the process a *permanent wave* (or perm). The process involved the alkaline borax softening the hair sufficiently to be remodeled, while the heating stiffened the borax to hold the hair into shape. The low cost of borax meant that Nessler's method was an immediate success.

### 6.5.2.2.2 Metaboric acid

Heating boric acid results in the partial dehydration to yield metaboric acid,  $\text{HBO}_2$ , (6.29). Metaboric acid is also formed from the partial hydrolysis of  $\text{B}_2\text{O}_3$ .



If the heating is carried out below  $130\text{ }^\circ\text{C}$ ,  $\text{HBO}_2$ -III is formed in which  $\text{B}_3\text{O}_3$  rings are joined by hydrogen bonding to the hydroxide on each boron atom (Figure 6.38). Continued heating to  $150\text{ }^\circ\text{C}$  results in  $\text{HBO}_2$ -II, whose structure consists of  $\text{BO}_4$  tetrahedra and  $\text{B}_2\text{O}_5$  groups chain linked by hydrogen bonding. Finally, heating above  $150\text{ }^\circ\text{C}$  yields cubic  $\text{HBO}_2$ -I with all the boron atoms tetrahedral.

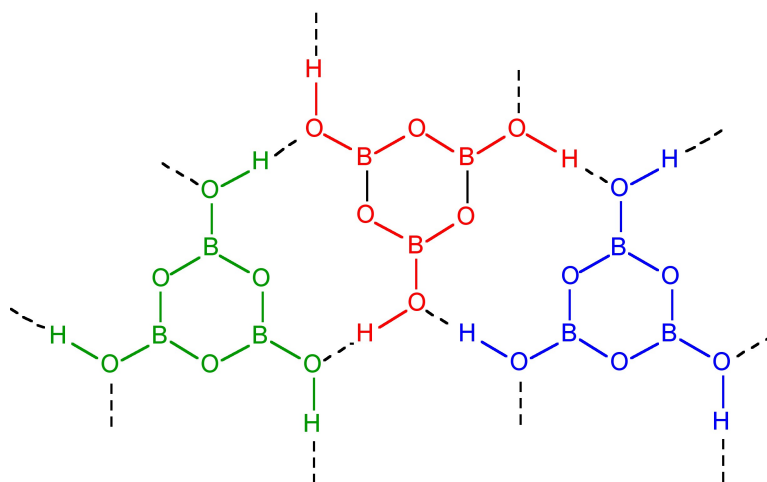


**Figure 6.38:** Structure of the layered structure of  $\text{HBO}_2$ -III.

### 6.5.2.3 Borate esters

Boric acid reacts with alcohols in the presence of sulfuric acid to form  $\text{B(OR)}_3$  (Figure 6.34). This is the basis for a simple flame test for boron. Treatment of a compound with methanol/sulfuric acid, followed by placing the reaction product in a flame results in a green flame due to  $\text{B(OMe)}_3$ .

In the presence of diols, polyols, or polysaccharides, boric acid reacts to form alkoxide complexes. In the case of diols, the mono-diol  $[\text{B(OH)}_2\text{L}]^-$  (Figure 6.39a) and the bis-diol  $[\text{BL}_2]^-$  (Figure 6.39b) complexes.

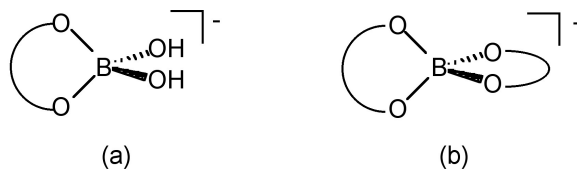


**Figure 6.39:** Structure of (a) the  $[\text{B}(\text{OH})_2\text{L}]^-$  and (b) the  $[\text{BL}_2]^-$  anions formed by the reaction of boric acid (or borate) with a diol.

Originally it was proposed that diols react with the anion rather than boric acid, (6.30). In contrast, it was suggested that the optimum pH for the formation of carboxylic acid complexes is under the condition where  $\text{pK}_a$  (carboxylic acid)  $<$   $\text{pH} <$   $\text{pK}_a$  (boric acid). Under these conditions it is the boric acid,  $\text{B}(\text{OH})_3$ , not the borate anion,  $[\text{B}(\text{OH})_4]^-$ , that reacts to form the complex.



The conversion of boric acid to borate ((6.23)) must occur through attack of hydroxide or the deprotonation of a coordinated water ligand, either of which is related to the  $\text{pK}_a$  of water. The formation of  $[\text{B}(\text{OH})_2\text{L}]^-$  from  $\text{B}(\text{OH})_3$  would be expected therefore to occur via a similar initial reaction (attack by  $\text{RO}^-$  or deprotonation of coordinated  $\text{ROH}$ ) followed by a subsequent elimination of  $\text{H}_2\text{O}$  and the formation of a chelate coordination, and would therefore be related to the  $\text{pK}_a$  of the alcohol. Thus the pH at which  $[\text{B}(\text{OH})_2\text{L}]^-$  is formed relative to  $[\text{B}(\text{OH})_4]^-$  will depend on the relative acidity of the alcohol. The  $\text{pK}_a$  of a simple alcohol (e.g.,  $\text{MeOH} = 15.5$ ,  $\text{EtOH} = 15.9$ ) are close to the value for water (15.7) and the lowest pH at which  $[\text{B}(\text{OH})_2\text{L}]^-$  is formed should be comparable to that at which  $[\text{B}(\text{OH})_4]^-$  forms. Thus, the formation of  $[\text{B}(\text{OH})_2\text{L}]^-$  as compared to  $[\text{B}(\text{OH})_4]^-$  is a competition between the reaction of  $\text{B}(\text{OH})_3$  with  $\text{RO}^-$  and  $\text{OH}^-$  (Figure 6.40), and as with carboxylic acids it is boric acid not borate that reacts with the alcohol, (6.31).



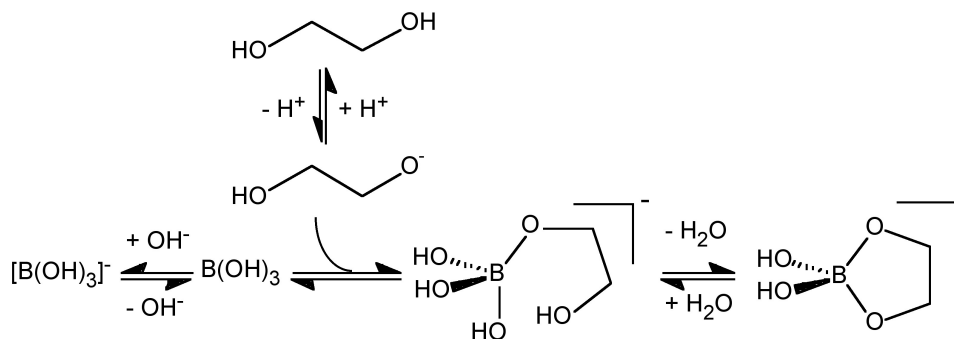


**Figure 6.40:** Competition between hydroxide and 1,2-diol for complexation to boron in the aqueous boric acid/diol system.

A key issue in the structural characterization and understanding of the diol/boric acid system is the assignment of the  $^{11}\text{B}$  NMR spectral shifts associated with various complexes. A graphical representation of the observed shift ranges for boric acid chelate systems is shown in Figure 6.41.

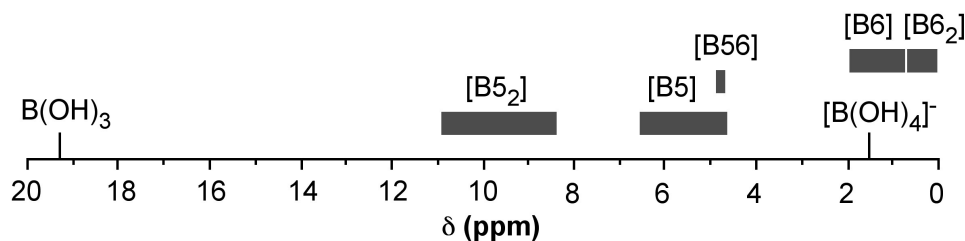


**Figure 6.41:**  $^{11}\text{B}$  NMR spectroscopic shifts of chelate alkoxide compounds in comparison with boric acid and borate anion. The acronyms [B5] and [B6] are used to denote a borate complex of a 1,2-diol and 1,3-diol forming a chelate 5-membered and 6-membered ring cycle, respectively. Similarly, [B5<sub>2</sub>] and [B6<sub>2</sub>] denotes a borate complex of two 1,2-diols or 1,3-diols both forming [BL<sub>2</sub>]<sup>-</sup>. Adapted from M. Bishop, N. Shahid, J. Yang, and A. R. Barron, *Dalton Trans.*, 2004, 2621.

### 6.5.2.3.1 Boric acid cross-linking of guar gum for hydraulic fracturing fluids

Thick gels of guar gum cross-linked with borax or a transition metal complex are used in the oil well drilling industry as hydraulic fracturing fluids. The polysaccharide guaran ( $M_w \approx 10^6$  Da) is the major (>85 wt%) component of guar gum, and consists of a (1→4)- $\beta$ -D-mannopyranosyl backbone with  $\alpha$ -D-galactopyranosyl side chain units attached via (1→6) linkages. Although the exact ratio varies between different crops of guar gum the general structure is consistent with about one galactose to every other mannose (Figure 6.42).